

Strong anisotropy effect in iron-based superconductor $\text{CaFe}_{0.882}\text{Co}_{0.118}\text{AsF}$

Yonghui Ma,^{1,2,3} Qiucheng Ji,^{1,2,3} Kangkang Hu,^{1,4} Bo Gao,¹ Wei Li,^{1,2,5,*} Gang Mu,^{1,2,†} and Xiaoming Xie^{1,2}

¹State Key Laboratory of Functional Materials for Informatics,
Shanghai Institute of Microsystem and Information Technology,
Chinese Academy of Sciences, Shanghai 200050, China

²CAS Center for Excellence in Superconducting Electronics(CENSE), Shanghai 200050, China

³University of Chinese Academy of Science, Beijing 100049, China

⁴Shanghai Key Laboratory of High Temperature Superconductors, Shanghai University, Shanghai 200444, China

⁵Department of Physics and State Key Laboratory of Surface Physics, Fudan University, Shanghai 200433, China

The anisotropy of the Fe-based superconductors is much smaller than that of the cuprates and the theoretical calculations. A credible understanding for this experimental fact is still lacking up to now. Here we experimentally study the magnetic-field-angle dependence of electronic resistivity in the superconducting phase of iron-based superconductor $\text{CaFe}_{0.882}\text{Co}_{0.118}\text{AsF}$, and find the strongest anisotropy effect of the upper critical field among the iron-based superconductors based on the framework of Ginzburg-Landau theory. The evidences of energy band structure and charge density distribution from electronic structure calculations demonstrate that the observed strong anisotropic effect mainly comes from the strong ionic bonding in between the ions of Ca^{2+} and F^- , which weakens the interlayer coupling between the layers of FeAs and CaF. This finding provides a significant insight into the nature of experimentally observed strong anisotropic effect of electronic resistivity, and also paves an avenue to design exotic two dimensional artificial unconventional superconductors in future.

Keywords: $\text{CaFe}_{0.882}\text{Co}_{0.118}\text{AsF}$, Fe-based Superconductors, Anisotropy

I. INTRODUCTION

Since the discovery of superconductivity of 26 K in fluorine doped quaternary compound LaFeAsO ,¹ the studies of the mechanism of iron-based superconductors (FeSCs) have evoked enormous interests across the community of superconductivity and material science. Huge experiments have revealed that the iron-based superconductors belong to a family of an unconventional pairing mechanism within layered FeAs(Se). The information of upper critical field H_{c2} and its anisotropy in superconductivity can be used as a fingerprint to understand the unconventional superconducting mechanism and to promote the practical applications.²⁻⁴ In addition, bidimensionality, which is represented by a rather high anisotropy between the ab -plane and c direction, is believed to be a very important factor for the occurrence of strong correlation physics and even high- T_c superconductivity⁵⁻⁹. Generally speaking, the anisotropy parameter γ of the FeSCs was found to be much smaller than that of the cuprates and the theoretical calculations.^{8,10-16} Although the Pauli-limit effects have been taken into account in well understanding the low temperature behaviors of H_{c2} ,¹⁷⁻¹⁹ the nature of such small value of anisotropy parameter γ of FeSCs remains unclear in the vicinity of superconducting (SC) transition temperature T_c . Interestingly, it has been found that the values of $\ln(\gamma^2)$ is linearly proportional to the distance d of adjacent conducting layers for both the cuprates superconductors and FeSCs,^{8,11} which is understandable since a thicker insulating block layer weakens the interlayer hybridization, as a result the anisotropy will be enhanced. Quantitatively, the value γ^2 of FeSCs has a magnitude typically two orders lower than that of cuprates superconductors

with the same d .

Recently, high-quality single crystals of CaFeAsF and the Co-doped compounds with the size above 1 mm were grown successfully by our group using a new flux CaAs ,^{20,21} which facilitates our research on the anisotropy effect of this system. Although the anisotropy parameter of the penetration depth were investigated by torque measurements previously,^{22,23} it was found that the value of γ obtained from London penetration depth experiment is quite different from that based on the upper critical field in FeSCs.^{24,25} The nature of such difference remains unclear. Motivated by this issue, we systematically study the anisotropy of the superconducting single crystals $\text{CaFe}_{0.882}\text{Co}_{0.118}\text{AsF}$ based on the upper critical fields. The magnetic-field-angular dependence of electronic resistivity in the superconducting state is measured and the results are found to follow the scaling law of the anisotropic Ginzburg-Landau (G-L) theory. The fitted anisotropy parameter is clearly larger than that of other FeSCs, and reaches the order of magnitude of the theoretical estimations.¹⁶ Based on the charge density distributions calculations, it is found that this strange phenomena mainly stems from the nature of the strong ionic bonding in between the ions of Ca^{2+} and F^- , which weakens the interlayer coupling between the FeAs and CaF layers.

II. EXPERIMENTAL DETAILS AND CALCULATIONS

The $\text{CaFe}_{1-x}\text{Co}_x\text{AsF}$ single crystals were grown using the CaAs self-flux method.^{20,21} The crystal structure and lattice constants of the materials were examined by

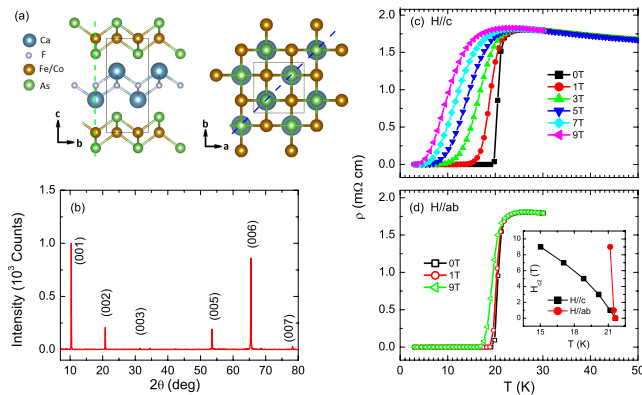


FIG. 1: (a) The schematic crystal structure of $\text{CaFe}_{1-x}\text{Co}_x\text{AsF}$ on (100) and (001) planes. The green and blue dashed lines denote the (010) and (110) planes where the charge density distribution was calculated (see Fig. 3). (b) X-ray diffraction pattern measured on the single crystal $\text{CaFe}_{0.882}\text{Co}_{0.118}\text{AsF}$ with the incident of x-ray on the ab -plane. (c)-(d) The electronic resistivity as a function of temperature under the magnetic field up to 9 T with $H//c$ and $H//ab$, respectively. The inset of (d) shows the upper critical fields H_{c2} as a function of temperature for two different orientations.

a DX-2700 type powder x-ray diffractometer using $\text{Cu K}\alpha$ radiation. The electronic resistivity (including the magnetic field angle-resolved electronic resistivity) were measured using a four probe technique on the physical property measurement system (Quantum Design, PPMS) with magnetic field up to 9 T. The angle φ was varied from 0° to 180° , where $\varphi = 0^\circ$ indicates the orientation with the magnetic field parallel to the c -axis of the sample. In addition, the current was applied always perpendicular to the direction of magnetic field, as shown schematically in the inset of Fig. 2(a).

The first-principles calculations presented in this work were performed using the all-electron full potential linear augmented plane wave plus local orbitals (FP-LAPW + lo) method²⁶ as implemented in the WIEN2K code.²⁷ The exchange-correlation potential was calculated using the generalized gradient approximation (GGA) as proposed by Pedrew, Burke, and Ernzerhof.²⁸ These calculations were performed using the experimental crystal structure²⁰, as shown in Fig. 1(a).

III. RESULTS

The x-ray was incident on the ab -plane of the sample when carrying out the x-ray diffraction measurements. The diffraction pattern is shown in Fig. 1(b), which follows the tetragonal ZrCuSiAs -type structure. It is important to point out that only the sharp peaks along the (00 l) orientation are observed, suggesting a high c -axis orientation. The actual doping level of cobalt was

determined to be 0.118 by the energy dispersive x-ray spectroscopy. Detailed analysis and discussions about the crystal structure and the chemical composition have been reported in our previous paper.²¹ Temperature dependence of electronic resistivity is shown in Fig. 1(c) and (d). Under zero field, the sample exhibits a sharp SC transition at $T_c(\text{onset}) = 21.6$ K ($90\%\rho_n$) with a transition width $\Delta T_c = 1.7$ K ($10\%-90\%\rho_n$), where ρ_n is the resistivity of the normal state before the SC transition, demonstrating the high quality of our single crystal samples. The slightly semiconducting behavior just above T_c along with the T_c value indicates that the present sample locates on the slightly underdoped region near the optimal doped point of the phase diagram.

We perform the measurements of temperature dependent electronic resistivity with the magnetic field along various orientations to study the anisotropy effect of H_{c2} of superconductor $\text{CaFe}_{1-x}\text{Co}_x\text{AsF}$. As shown in Fig. 1(c) and (d), the SC transition point shifts to lower temperature with the increase of the magnetic field for both the orientations of parallel and perpendicular to c -axis of the crystal structure. It is worthy to note that the SC transition for the orientation of $H//c$ shifts much quicker than that of $H\perp c$ by comparing the data from Fig. 1(c) and (d). Quantitatively, we use $90\%\rho_n$ to determine the upper critical field H_{c2} . The temperature dependence of H_{c2} is shown in the inset of Fig. 1(d) for both the two orientations, and the value of anisotropy parameter is estimated to be $\gamma = H_{c2}^{ab}/H_{c2}^c = 9$ at temperature of 21.2 K.

To gain more information about the anisotropy effect of H_{c2} , we further measure the magnetic-field-angle dependence of electronic resistivity under various magnetic fields at the temperature region near the SC transition point. Here we take the data at the temperature of 19 K as an example and plot it in Fig. 2(a). In addition, the schematic illustration of applied magnetic field and the dc current is also shown in the inset of Fig. 2(a). The positive magnetoresistivity displays a V-shaped structure with occurring the minimum at $\varphi = 90^\circ$ and maximum at $\varphi = 0^\circ$ and $\varphi = 180^\circ$. Similar results are also obtained for other temperatures indicating the universal behaviours of magnetic-field-angle dependent magnetoresistivity. Based on the anisotropic GL theory, the effective upper critical field as a function of the orientation of azimuth angle φ is expressed as²⁹:

$$H_{c2}^{GL}(\varphi) = \frac{H_{c2}^{ab}}{\sqrt{\sin^2\varphi + \gamma^2\cos^2\varphi}} \propto \frac{1}{\sqrt{\sin^2\varphi + \gamma^2\cos^2\varphi}}. \quad (1)$$

Here, it should be noted that the resistivity in the superconducting state merely depends on the effective magnetic field H/H_{c2}^{GL} , i.e., $\rho = \rho[H/H_{c2}^{GL}(\varphi)]$, at a given temperature.³⁰ According to the Eq. (1), we rewrite the resistivity as a function of $H\sqrt{\sin^2\varphi + \gamma^2\cos^2\varphi}$, and show it in Fig. 2(b). It clearly demonstrates the universal behaviors that all magnetic field dependent electronic resistivity

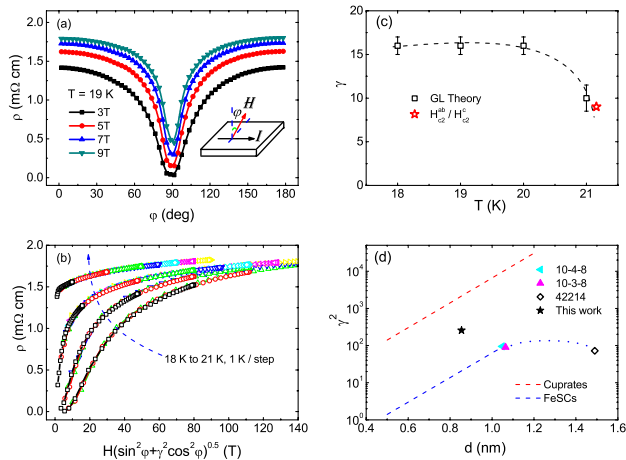


FIG. 2: (a) Magnetic field angular-dependence of electronic resistivity at 19 K under magnetic fields up to 9 T. The inset illustrates schematically the definition of angle φ , and the electron current is always perpendicular to the magnetic field. (b) Scaled resistivity at 18 K, 19 K, 20 K and 21 K as a function of $H(\sin^2 \varphi + \gamma^2 \cos^2 \varphi)^{0.5}$. (c) Temperature dependence of the anisotropy parameters γ obtained from the GL theory and H_{c2}^{ab}/H_{c2}^c . (d) Comparing our result of anisotropy with other FeSCs and cuprates. Here γ^2 is extracted at the temperature $0.85T_c$ and d is the distance of the neighboring conducting layers. The two dashed lines representing the tendency of the previously reported FeSCs and cuprates superconductors are cited from Ref. [11]. The value of the 42214 system was reported in Ref. [31], which implies a saturated tendency as d becomes even larger.

tivity falls into one curve at a fixed temperature. In addition, temperature dependence of the fitted anisotropic parameter γ is also shown in Fig. 1(c). For a comparison, we also show a consistent value of anisotropic parameter γ estimated from H_{c2}^{ab}/H_{c2}^c . Importantly, these anisotropic values are much larger than that reported on other FeSCs.

In Fig. 2(d), we also show the γ^2 values at $0.85 T_c$ as a function of the distance d between the neighboring conducting layers (FeAs layers or CuO_2 layers). The two dashed lines, respectively, represent the tendency of the previously reported FeSCs and cuprates superconductors.¹¹ Generally speaking, the value of γ^2 for FeSCs is two orders of magnitude lower than that of cuprates superconductors with the same value of d . Exceptionally, the value of $\text{CaFe}_{0.882}\text{Co}_{0.118}\text{AsF}$ locates above the blue dashed line which indicates a common tendency of FeSCs, and even higher than the 10-3-8, 10-4-8 and 42214 systems $[\text{Ca}_{10}(\text{Pt}_n\text{As}_8)(\text{Fe}_{2-x}\text{Pt}_x\text{As}_2)_5$ ($n = 3, 4$), $\text{Pr}_4\text{Fe}_2\text{As}_2\text{Te}_{1-x}\text{O}_4$] with a much larger space between the FeAs layers.^{11,31}

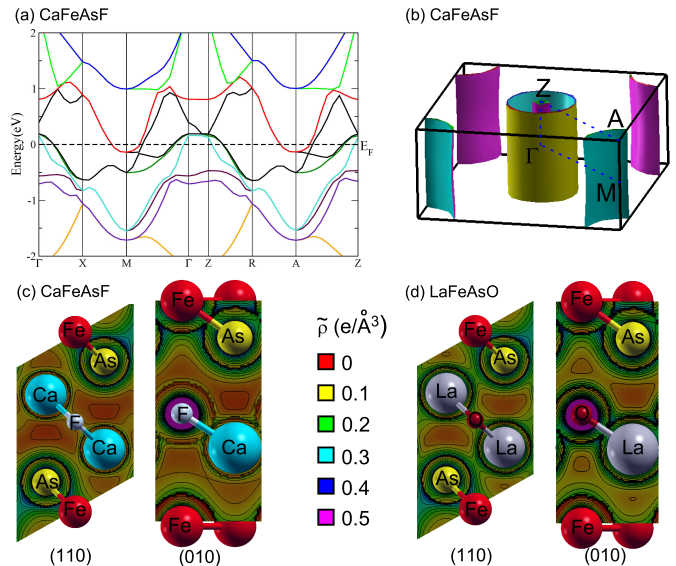


FIG. 3: (a) Calculated band structure of CaFeAsF . The Fermi energy was set to zero (dashed line). There is no band intersecting the Fermi level between the Γ and Z points. (b) The Fermi surfaces of CaFeAsF . (c)-(d) Charge density distribution ($\tilde{\rho}$) of the (110) and (010) planes for CaFeAsF and LaFeAsO respectively.

IV. DISCUSSION

Although we have found the largest anisotropy parameter γ of $\text{CaFe}_{0.882}\text{Co}_{0.118}\text{AsF}$ in iron-based superconductors, the experimental observation is consistent with the theoretical prediction by the first-principles calculations. Previously, D. J. Singh *et al*¹⁶ predicted the anisotropy to be about 15 for the parent phase of the 1111 system after the discovery of the high- T_c FeSCs. Since the anisotropy is tightly related to the electronic structure, and as we known that the Fermi surface of FeSCs consists of five sheets, where two electron-like cylinders centered around the M-A line and two hole-like cylinders around the Γ -Z line, as well as an additional small 3D hole-like pocket centered at Z point, individual characters in details of the electronic structure may have remarkable influences on the anisotropic effect of the materials, such as the strong warping of the electron pockets in the 122, 111, and 11 systems, compared with the 1111 system,^{16,32,33} can be expected to increase the tendency of 3D characterizations, which may explain the fact that the anisotropy parameter of these three systems is smaller than of the 1111 system.

In order to examine the detailed electronic structure of $\text{CaFe}_{0.882}\text{Co}_{0.118}\text{AsF}$ and clarify the nature of the emergence of strongest electronic anisotropy among the FeSCs, we carried out the first-principles calculations. The electronic band structure should be changed slightly by the cobalt doping of 11.8% based on the rigid-band approximation. For simplicity, we just only show the en-

ergy band and its Fermi surface topology of CaFeAsF in Fig. 3(a) and (b), respectively, which are in good agreement with previous report.³⁴ Firstly we examine the energy dispersions between high symmetric \mathbf{k} -points of Γ and Z , there is no band intersects across the Fermi level. This result indicates the absence of the 3D Fermi pocket around the Z point. In addition, it is found that all of the Fermi surface sheets are almost ideal cylinders [see Fig. 3(b)]. Previously, I. A. Nekrasov *et al* have pointed out that the fluorine-based 1111 system displays a much more perfect 2D character of the Fermi surfaces than the oxygen-based 1111 system LaFeAsO³⁵. As for the compounds with an even larger interlayer distance like the 10-3-8 system, both the ARPES measurements and first-principles calculations have demonstrated a strong 3D character in the topology of the Fermi surface stemming from the strong hybridization with the Pt d_{z^2} orbitals.³⁶ This should definitely suppress the bidimensionality of the Fermi surface. The perfect bidimensionality of CaFeAsF may explain the experimental fact of the strong anisotropy of CaFe_{0.882}Co_{0.118}AsF qualitatively.

Quantatively, we calculated the charge density distribution, $\tilde{\rho}(r)$, as shown in Fig. 3(c). For comparison, we also performed the charge density distribution $\tilde{\rho}(r)$ calculation for the system of LaFeAsO with the same crystal structure of CaFeAsF and shown in Fig. 3(d). From the distribution of $\tilde{\rho}(r)$ in the (110) plane, it displays no difference of the $\tilde{\rho}(r)$ around Fe-As bond between LaFeAsO and CaFeAsF, but the $\tilde{\rho}(r)$ in the area of La-As has clearly much higher value than that in the area of Ca-As, suggesting the weakness of the interlayer coupling between the layers of FeAs and CaF. This result is also understandable because the strong electronegativity of F favors to form the much stronger ionic binding with Ca, as revealed by the lower values of $\tilde{\rho}(r)$ in between Ca²⁺ and F⁻ ions in the (010) plane, and weakens the inter-

layer coupling. This mechanism well explains the nature of such a strong electronic anisotropy observed in experiments in the system of CaFeAsF.

V. CONCLUSIONS

In summary, magnetic field angular dependence of resistivity in the superconducting state was measured on the single crystals of CaFe_{0.882}Co_{0.118}AsF. The obtained anisotropy parameter γ based on the anisotropic Ginzburg-Landau theory is much larger than that of other FeSCs. By the charge density distribution calculations, we found that the strong electronic anisotropy mainly comes from the strong intra-layer ionic bonding in CaF layer, which weakens the interlayer coupling between the layers of FeAs and CaF. Our results demonstrate that the fluorine-base 1111 system may be the most 2D superconducting material in FeSCs, from the viewpoint of electronic structure. The interplay between strong electronic anisotropy and unconventional superconductivity is an important issue for the understanding the mechanism of unconventional superconductor, which deserves our attentions in the future.

Acknowledgments

This work is supported by the National Natural Science Foundation of China (Nos. 11204338 and 11404359), the ‘‘Strategic Priority Research Program (B)’’ of the Chinese Academy of Sciences (Nos. XDB04040300, and XDB04030000) and Youth Innovation Promotion Association of the Chinese Academy of Sciences (Nos. 2015187 and 2016215).

* liwei@mail.sim.ac.cn

† mugang@mail.sim.ac.cn

¹ Y. Kamihara, T. Watanabe, M. Hirano and H. Hosono, *J. Am. Chem. Soc.* **130**, 3296 (2008).

² M. Putti, I. Pallecchi, E. Bellingeri, M. R. Cimberle, M. Tropeano, C. Ferdeghini, A. Palenzona, C. Tarantini, A. Yamamoto, J. Jiang, J. Jaroszynski, F. Kametani, D. Abaimov, A. Polyanskii, J. D. Weiss, E. E. Hellstrom, A. Gurevich, D. C. Larbalestier, R. Jin, B. C. Sales, A. S. Sefat, M. A. McGuire, D. Mandrus, P. Cheng, Y. Jia, H. H. Wen, S. Lee and C. B. Eom, *Supercond. Sci. Technol.* **23**, 034003 (2010).

³ H. Hosono, K. Tanabe, E. T. Muromachi, H. Kageyama, S. Yamanaka, H. Kumakura, M. Nohara, H. Hiramatsu and S. Fujitsu, *Sci. Technol. Adv. Mater.* **16**, 033503 (2015).

⁴ V. G. Kogan and R. Prozorov, *Rep. Prog. Phys.* **75**, 114502 (2012).

⁵ J. A. Wilson, F. J. Di Salvo, and S. Mahajan, *Adv. Phys.* **24**, 117 (1975).

⁶ G. Grüner, *Rev. Mod. Phys.* **60**, 1129 (1988).

⁷ C. Cruz, Q. Huang, J. W. Lynn, J. Li, W. Ratcliff, J. L. Zarestky, A. H. Mook, G. F. Chen, J. L. Luo, N. I. Wang, P. C. Dai, *Nature* **453**, 899 (2008).

⁸ J. Shimoyama, K. Kitazawa, K. Shimizu, S. Ueda, S. Horii, N. Chikumoto and K. Kishio, *Low Temp. Phys.* **131**, 1043 (2003).

⁹ K. Zhao, B. Lv, Y. Xue, X. Zhu, L. Deng, Z. Wu, and C. W. Chu, *Phys. Rev. B* **92**, 174404 (2015).

¹⁰ Y. Jia, P. Cheng, L. Fang, H. Yang, C. Ren, L. Shan, C. Z. Gu and H. H. Wen, *Supercond. Sci. Technol.* **21**, 105018 (2008).

¹¹ F. F. Yuan, Y. Sun, W. Zhou, X. Zhou, Q. P. Ding, K. Iida, R. Hühne, L. Schultz, T. Tamegai and Z. X. Shi, *Appl. Phys. Lett.* **107**, 012602 (2015).

¹² S. Khim, B. Lee, J. W. Kim, E. S. Choi, G. R. Stewart and K. H. Kim, *Phys. Rev. B* **84**, 104502 (2011).

¹³ M. H. Fang, J. H. Yang, F. F. Balakirev, Y. Kohama, J. Singleton, B. Qian, Z. Q. Mao, H. D. Wang and H. Q. Yuan, *Phys. Rev. B* **81**, 020509 (2010).

¹⁴ F. F. Yuan, K. Iida, M. Langer, J. Hänisch, A. Ichinose, I.

- Tsukada, A. Sala, M. Putti, R. Hühne, L. Schultz and Z. X. Shi, *Supercond. Sci. Technol.* **28**, 065005 (2015).
- ¹⁵ Y. Sun, T. Taen, Y. Tsuchiya, Q. P. Ding, S. Pyon, Z. X. Shi and T. Tamegai, *Appl. Phys. Express* **6**, 043101 (2013).
- ¹⁶ D. J. Singh and M. H. Du, *Phys. Rev. Lett.* **100**, 237003 (2008).
- ¹⁷ S. Khim, B. Lee, J. W. Kim, E. S. Choi, G. R. Stewart and K. H. Kim, *Phys. Rev. B* **84**, 104502 (2011).
- ¹⁸ G. Fuchs, S. L. Drechsler, N. Kozlova, M. Bartkowiak, G. Behr, K. Nenkov, H. H. Klauss, J. Freudenberger, M. Knupfer, F. Hammerath, G. Lang, H. J. Grafe, B. Buechner and L. Schultz, *Physica C* **470**, S288 (2010).
- ¹⁹ S. Zhang, Y. P. Singh, X. Y. Huang, X. J. Chen, M. Dzero and C. C. Almasan, *Phys. Rev. B* **92**, 174524 (2015).
- ²⁰ Y. H. Ma, H. Zhang, B. Gao, K. K. Hu, Q. C. Ji, G. Mu, F. Q. Huang and X. M. Xie, *Supercond. Sci. Technol.* **28**, 085008 (2015).
- ²¹ Y. H. Ma, K. K. Hu, Q. C. Ji, B. Gao, H. Zhang, G. Mu, F. Q. Huang and X. M. Xie, *Journal of Crystal Growth* **451**, 161 (2016).
- ²² H. Xiao, B. Gao, Y. H. Ma, X. J. Li, G. Mu and T. Hu, *J. Phys.: Condens. Matter* **28**, 455701 (2016).
- ²³ H. Xiao, B. Gao, Y. H. Ma, X. J. Li, G. Mu and T. Hu, *J. Phys.: Condens. Matter* **28**, 325701 (2016).
- ²⁴ S. Weyeneth, R. Puzniak, N. D. Zhigadlo, S. Katrych, Z. Bukowski, J. Karpinski and H. Keller, *J Supercond Nov Magn* **22**, 347-351 (2009).
- ²⁵ M. Bendele, S. Weyeneth, R. Puzniak, A. Maisuradze, E. Pomjakushina, K. Conder, V. Pomjakushin, H. Luetkens, S. Katrych, A. Wisniewski, R. Khasanov, and H. Keller, *Phys. Rev. B* **81**, 224520 (2010).
- ²⁶ D. J. Singh and L. Nordstrom, *Planewaves, Pseudopotentials, and the LAPW Method*, 2nd ed. (Springer-Verlag, Berlin, 2006).
- ²⁷ P. Blaha, K. Schwarz, G. Madsen, D. Kvasnicka, and J. Luitz, in *WIEN2K, An Augmented PlaneWave + Local Orbitals Program for Calculating Crystal Properties*, edited by K. Schwarz (Technical University Wien, Austria, 2001).
- ²⁸ J. P. Perdew, K. Burke and M. Ernzerhof, *Phys. Rev. Lett.* **77**, 3865 (1996).
- ²⁹ G. Blatter, M. V. Feigel'man, V. B. Geshkenbein, A. I. Larkin and V. M. Vinokur, *Rev. Mod. Phys.* **66**, 1125 (1994).
- ³⁰ G. Blatter, V. B. Geshkenbein and A. I. Larkin, *Phys. Rev. Lett.* **68**, 875 (1992).
- ³¹ A. Pisoni, P. Szirmai, S. Katrych, B. Náfrádi, R. Gaál, J. Karpinski, and L. Forró, *Phys. Rev. B* **93**, 094519 (2016).
- ³² D. J. Singh, *Phys. Rev. B* **78**, 094511 (2008).
- ³³ B. Zeng, G. Mu, H. Luo, T. Xiang, I. I. Mazin, H. Yang, L. Shan, C. Ren, P. C. Dai and H. H. Wen, *Nat. Commun.* **1**, 112 (2010).
- ³⁴ I. R. Shein and A. L. Ivanovskii, *JETP Letters* **88**, 683 (2008).
- ³⁵ I. A. Nekrasov, Z. V. Pchelkina and M. V. Sadovskii, *JETP Letters* **88**, 679 (2008).
- ³⁶ M. Neupane, C. Liu, S. Y. Xu, Y. J. Wang, N. Ni, J. M. Allred, L. A. Wray, N. Alidoust, H. Lin, R. S. Markiewicz, A. Bansil, R. J. Cava, and M. Z. Hasan, *Phys. Rev. B* **85**, 094510 (2012).